Petrography, Geothermobarometry and Metamorphic History of Metapelites from the Central Ruby Range Southwest Montana

HAMELIN, Clémentine[1], BALDWIN, Julia A.[2], HARMS, Tekla A.[3], and BRADY, John B.[1]

[1] Department of Geosciences, Smith College, Northampton, MA 01063, chamelin@smith.edu, [2] Department of Geosciences, University of Montana, Missoula, MT 59812, [3] Department of Geology, Amherst College, Amherst, MA 01002

ABSTRACT

The Ruby Range is one of several uplifted Precambrian blocks in southwest Montana, near the northwestern margin of the Archean Wyoming province. It was metamorphosed during the Big Sky orogeny ~ 1.72-1.79 Ga (Baldwin et al., 2014; Cramer et al., 2013). This study seeks to characterize further the P-T metamorphic conditions of the Big Sky orogenic event as recorded in the central Ruby Range. Metapelite samples were collected during July 2014 as part of a Keck Geology Consortium summer research project. Garnet-biotite-sillimanite-bearing metapelite rocks associated with marble, amphibolite and metamorphosed banded iron formation were sampled from the Christensen Ranch Metamorphic Suite (CRMS) at the highest structural levels of the central Ruby Range near Stone Creek. Textures and mineral assemblages preserve evidence for partial melting. All samples contain the assemblage biotite + garnet + sillimanite +quartz, consistent with upper amphibolite facies metamorphism. Four samples were further investigated with petrographic observations, geochemical XRF and SEM/EDS analyses and modeling to determine *P-T* conditions and history recorded in the samples. A peak temperature of ~800°C at a pressure of 9kb was determined and a second, possibly re-equilibrated T,P value of ~700°C and ~ 7 kbar was calculated in one sample. Issues relating to water-content, melt-loss estimation in modeling as well as polymetamorphism still have to be fully addressed in order to fully understand the metamorphic history of the CRMS metapelites.

INTRODUCTION

- The Ruby Range is one of several Laramide uplifted blocks of exposed Precambrian basement in the Wyoming Province.
- Metamorphosed at 2.45 Ga and 1.72-1.79 Ga during the Big Sky Orogeny, (Harms et al., 2004; Cheney et al., 2004).
- This project examines metapelites along the Stone Creek drainage, from the structurally highest unit of the Ruby Range, the Christensen Ranch Metamorphic Suite (CRMS) overlying the Dillon Gneiss and Pre-Cherry Creek suite.
- CRMS only show Proterozoic monazite ages 1.72-1.79 Ga (Cramer et al., 2014)
- The purpose of this study is to determine metamorphism conditions of pressure and temperature recorded in these metapelites to further constrain and understand the Big Sky orogeny as recorded in the Ruby Range, complementing our understanding of this orogenic event studied in the adjacent mountain ranges such as the Tobacco Root Mountains or the Gravelly Range.
- Petrography, mineral chemistry and thermodynamic modeling.

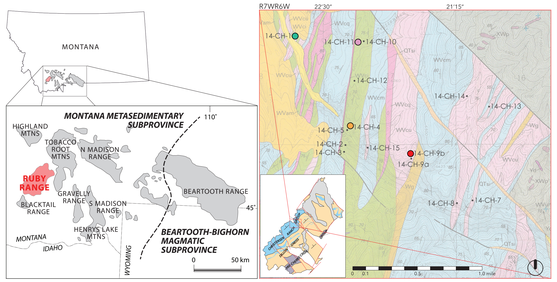

Figure 1. Sample distribution and location map along Stone Creek. Metapelite samples were generally sampled in the undifferentiated metasedimentary units (mapped in pink), a few samples were collected in the amphibolite unit (mapped in green). Other units mapped are calcitic and dolomitic marbles (blue), metamorphosed banded iron formation (purple) and quartzite (magenta). Note the contact with the Dillon gneisses (olive green) to the left of the map. (Modified from James, 1990).

METHODS

- 21 metapelite samples collected in the summer of 2014 during a KECK project, along Stone Creek traverse, structurally covering the base to the top of the Christensen Ranch Metamorphic Suite (Figure 1).
- All samples have mineral assemblage garnet + biotite + sillimanite + quartz. Outcrop and sample positions recorded in NAD 84 UTM coordinates using a GPS. Samples and field relationships with surrounding units were described in the field.

FOR PSEUDOSECTION GEOTHERMOBAROMETRY:

(1) 25 sections were made, phases, modes and reaction textures identified, described and quantified using a petrographic microscope.
(2) Bulk rock chemistry for major and trace elements (X-Ray Fluorescence, XRF) and REE (Inductively Coupled Plasma Mass Spectrometry, ICPMS) was obtained through Acme Labs, Vancouver Canada for 9 samples.
(3) 6 samples analyzed using and FEI Quanta 450 SEM with EDAX EDS. Garnet, biotite and plagioclase mineral chemistry was quantified, modal phase maps were generated.

- Pseudosection modeling for 9 samples in Na-Ca-K-Fe-Mg-Al-Si-H-Ti-O (NCKFMASHTO) system with TheriakDomino v. 03.08.2009 & pelites (Holland and Powell dataset 5.5), for LOI water value vs. H_2O determined using a T-X_{H2O} binary diagram calculated in Theriak Domino. No apatite correction was done, Mn was left out and small ferric iron values were used.
- Stable mineral assemblages, actual modes vs. calculated modes, and mineral compositions compared for LOI vs. T-X_{H2O} determined H_2O value

RESULTS

PETROGRAPHY

MINERAL ASSEMBLAGES
grt + bt + sill + pl + qtz ± ap ± k-spar ± chl ± mu ± ilm ± ru ± gr ± trm.

- Schistose texture with well-developed foliation defined by abundant biotite and sillimanite grain alignment. Two samples with a gneissic texture, with higher feldspar + quartz content.
- Garnets: anhedral, range in size from 1 mm to 10 cm diameter. Generally Fe-rich (~80% almandine), little to no zoning, but with evidence for two garnet-growth episodes (inclusion free or different rims, Ca and Fe zoning in one sample).
- Biotite Fe-Mg ratios in biotite range from ~ 1:1 to 2:3 across samples but generally consistent within samples.
- Generally muscovite-free, a few samples contain minor amounts of retrograde-muscovite.
- Kyanite and cordierite-absent.
- Most samples k-feldspar poor, only samples CH1, 9b and 11a contains abundant matrix k-feldspar.

PHASE MAPS - KEY

GARNET PLAG KSPAR MAGN RUTILE BIOTITE ILM SILL QTZ APAT

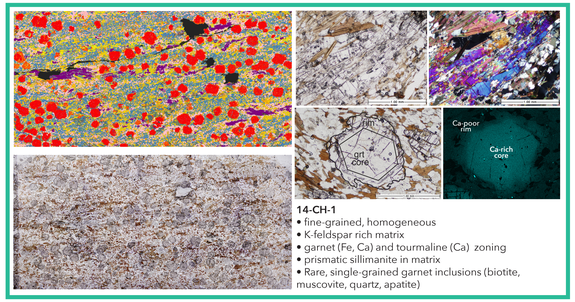

14-CH-1
- fine-grained, homogeneous
- K-feldspar rich matrix
- garnet (Fe, Ca) and tourmaline (Ca) zoning
- prismatic sillimanite in matrix
- Rare, single-grained garnet inclusions (biotite, muscovite, quartz, apatite)

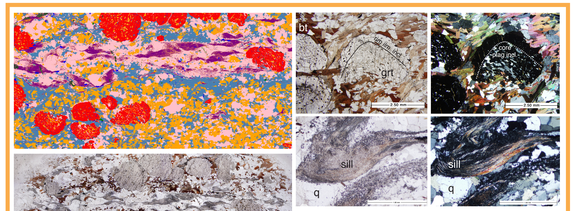

14-CH-4
- medium to coarse grained, poikiloblastic garnet clusters around quartz + sillimanite melt.
- No K-feldspar, no muscovite in matrix
- Flat garnet profiles, plagioclase inclusions in cores and ilmenite inclusions in rims or ears, strong inclusion trails.

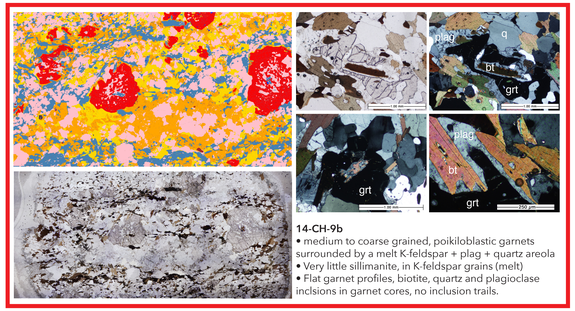

14-CH-9b
- medium to coarse grained, poikiloblastic garnets surrounded by a melt K-feldspar + plag + quartz areola
- Very little sillimanite, in K-feldspar grains (melt)
- Flat garnet profiles, biotite, quartz and plagioclase inclsions in garnet cores; no inclusion trails.

14-CH-11a
- fine grained, small anhedral Mn-rich garnets
- Abundant fibrous sillimanite bundles, localized K-feldspar-rich matrix layers vs. K-feldspar absent matrix layers, quartz-rich sample
- Mn-zoning in garnets, Mn-rich rims and Mn-poor cores
- Small quartz inclusions in garnet.

Figure 2. Sample Petrography: Phase maps, thin section maps and textural details. 2a) CH1 - top: prismatic sillimanite texture, PPL & XPL, bottom: two episodes of garnet growth, euhedral core and crinkled rim (XPL and Ca-zoning EDS map), 2b) CH4 - top: two garnet growth episodes, plagioclase-free, ilmenite-rich rim inclusions (PPL) and plagioclase-rich core inclusions (XPL), 2c) CH9b - garnet-biotite-lagioclase reaction textures (melting?), and 2d) CH11a - thin section photomicrograph in PPL, abundant sillimanite bundles along foliation, quartz-plag-K-feldspar rich matrix.

PSEUDOSECTION GEOTHERMOBAROMETRY

Figure 3. left column: pseudosections for samples CH1, CH4, CH9b and CH11a using water saturation at solidus determined using a T-X_{H2O} diagram for XRF bulk rock composition. central column: pseudosections using loss on ignition (LOI) water values, right column: T-X_{H2O} diagrams a 7.5 kbar showing variations due to water content adjustments. Pseudosections marked with isopleths corresponding to quantified mineral compositions for each sample. Darker ellipses show further P-T constraint based on approximate isopleth intersection.

PSEUDOSECTION ISOPLETHS
- Garnet Mg/(Mg+Fe)
- Biotite Mg/(Mg+Fe)
- Garnet grossular Ca/(Fe+Mg+Ca)
- Garnet almandine Fe/(Fe+Mg+Ca)
- Plagioclase anorthite Ca/(Ca+Na+K)

PSEUDOSECTION WATER SATURATION AT SOLIDUS

PSEUDOSECTION LOI WATER VALUE

T-X_{H2O} BINARY DIAGRAM LOI WATER VALUE VS. SATURATION AT SOLIDUS

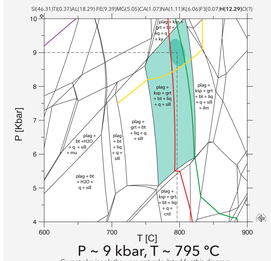

P ~ 9 kbar, T ~ 795 °C
Garnet alm isopleths were not calculated for this diagram

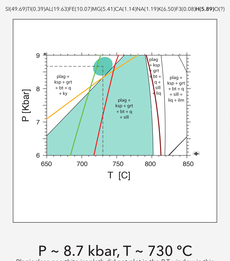

P ~ 8.7 kbar, T ~ 730 °C
Plagioclase anorthite isopleth did not plot in the *P-T* window in this diagram

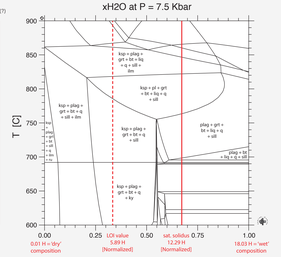

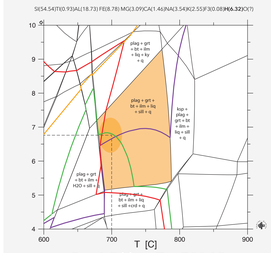

P ~ 6.8 kbar, T ~ 700 °C
Garnet alm isopleths were not calculated for this diagram

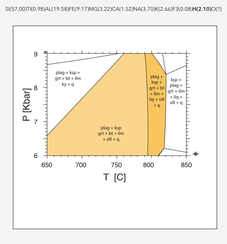

P ~ 6-9 kbar, T ~ 695-820 °C
None of the isopleths plotted in the *P-T* window in this diagram

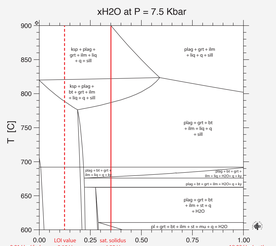

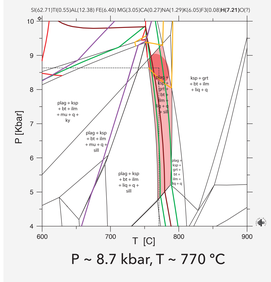

P ~ 8.7 kbar, T ~ 770 °C

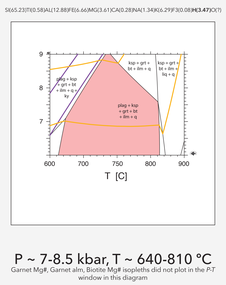

P ~ 7-8.5 kbar, T ~ 640-810 °C
Garnet Mg#, Garnet alm, Biotite Mg# isoplethis did not plot in the *P-T* window in this diagram

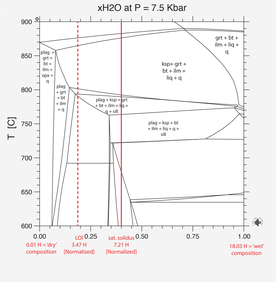

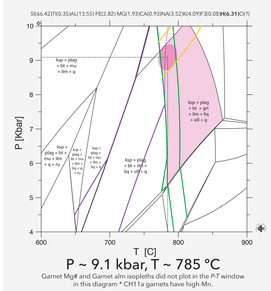

P ~ 9.1 kbar, T ~ 785 °C
Garnet Mg# and Garnet alm isopleths did not plot in the *P-T* window in this diagram * CH11a garnets have high-Mn.

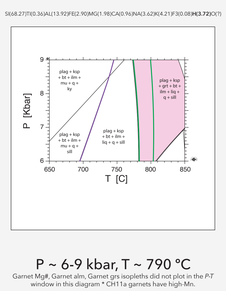

P ~ 6-9 kbar, T ~ 790 °C
Garnet Mg#, Garnet alm, Garnet grs isoplethis did not plot in the *P-T* window in this diagram * CH11a garnets have high-Mn.

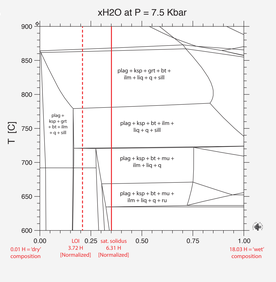

RESULTS

- Stable assemblage fields in mineral assemblage diagrams match petrography. Modeled (Theriak-Domino) vs. observed modes (SEM phase map) also match well for both LOI water value vs. H_2O saturation at solidus value (Table 1)
- Petrography: NKFMASH petrogenetic grid, preliminary constraints on *P,T* are 650 °C - 900 °C (muscovite-OUT, K-feldspar-IN), 2-11 kbar (cordierite and kyanite absent) (Figure 4, grey area).
- Further *P-T* constraint from pseudosection modeling, from both LOI diagrams and added water diagrams to ~750-800 °C and 7-9 kb (Figure 4), Peak-T at ~800 °C
- In general, isopleths for biotite (Mg#), garnet (Mg#, alm, gr) and plagioclase (Ca) match better on H_2O diagrams vs. LOI diagrams.
- Overall, results from pseudosection modeling consistent with mineral compositional analyses and determined modes, with some differences within *P-T* window (lower *P,T* vs. higher *P,T*)

PHASE	GARNET			BIOTITE			SILL.			QUARTZ			PLAG.			K-SPAR			ILMENITE		
modes(vol%)	LOI	H2O+	ROCK	LOI	H2O+	ROCK	LOI	H2O+	ROCK	LOI	H2O+	ROCK	LOI	H2O+	ROCK	LOI	H2O+	ROCK	LOI	H2O+	ROCK
CH1	17	16	19	28	33	31	3	5	3	23	24	21	10	8	7	20	16	17	0	0	0
CH4	18	12	13	10	19	23	5	6	5	31	33	30	28	26	24	7	0	0	1.4	1.2	0.7
CH9b	10	4	11	15	23	18	0	0.4	0.1	44	46	32	7	7	23	27	16	15	0.5	0.3	0.1
CH11a	1.6	1.4	1	12	12	10	3	3	5	47	46	50	23	23	20	11	11	10	0.3	<1	<1

Table 1. Phase mode comparison in samples for calculated LOI and H2O melt saturation at solidus modeling, and quantified phase modes (SEM/EDS phase map for CH1, CH4, CH9b; estimated modes for CH11a).

DISCUSSION

- Results plotted on NCKFMASH grid, within consistent range, but with some differences, which could be due to polymetamorphism (evidence for multiple episodes of garnet growth & consumption).
- All CRMS ages 1.72-1.79 Ga: *P-T* conditions recorded for Big Sky orogeny in the Ruby Range, not from metamorphic events at 2.45 Ga.

MODELING ISSUES & SOURCES OF DISCREPANCIES IN RESULTS

- Sources of error: a-x models, no Mn, no apatite correction, composition analyses, H_2O content, melt loss, polymeta morphism.
- What is more representative of these rocks, If assume H_2O loss from dehydration melting reactions only? (Spear et al., 1999)
- Melt-loss not represented in the bulk rock chemistry: compositions representative of post-melt loss conditions and possible reequilibration temperatures (CH4) vs. pre-melt loss, peak-T conditions (CH1)?

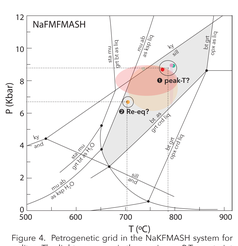

Figure 4. Petrogenetic grid in the NaKFMASH system for pelites. The light grey area is the maximum *P-T* constraint obtained from petrographic observations (mineral reactions and mineral assemblage), while the colored spots show *P-T* constraints determined by pseudosection modeling (Modified from Spear et al.,1999).

CONCLUSION & SIGNIFICANCE

- Implications for the Big Sky orogeny in the Ruby Range: constraint on peak temperature of ~800 °C at pressure of ~9 kbar.
- Calculated requilibrium temperature of ~700 °C at pressure of ~7 kbar.
- Calculation results affected bulk rock composition H_2O content estimations, mineral composition measurements, mineral a-x models, melt loss and polymetamorphism.
- Result for peak-T for the Big Sky orogeny comaprable to result in the Tobacco Root Mountains, recorded in pelitic schists from the Indian Creek Metasedimentary Suite (Cheney et al., 2004).

ACKNOWLEDGEMENTS

I would like to thank my advisor, John B. Brady, for putting the time and energy in this project, for letting me make my own decisions about this research and giving me a sense of ownership in the work I am doing, making this an intensive learning and growing collaborative research experience. I am also extremely thankful to Julia A. Baldwin, for helping me with the Theriak Domino modeling and for giving me precious advice on how to think about rocks in the Ruby Range, in the field and in the lab. I would also like to thank Tekla A. Harms for her patience and understanding with technical issues, and here eternal support and motivation to keep going and not get discouraged. I would also like to thank Jack Cheney for taking time to stain my rocks for K-feldspar at Amherst, Mike Vollinger for the cookies, and for helping me bypass the persistant admin password barrier on college computers, and doing so on many, repeated occasions, as well as Judith Whopereis for her help and technical support with the SEM/EDS system. Finally, I would like to thank the KECK Geology Consortium and the Ruby Rangers, for making exciting research in the field and in the lab possible, and for fun times in Montana!

REFERENCES

- Baldwin, J.A., Cramer, M.A., Voarino, B., 2014, Late Archean to Paleoproterozoic evolution of the Ruby Range, Montana, and its implications for the growth and modification of the Northwestern Wyoming Province: Geological Society of America Abstracts with Programs, v. 46, No 5, p. 20.
- Cheney, J.T., Brady, J.B., *Tierney, K.A., *DeGraff, K.A., *Mohlman, H.K., *Frisch, J.D., *Hatch, C.E., *Horner, M.L., *Tuit, C., *Steffan, K.J., *Cady, P., *Lowell, J., *Archuleta, L.L., *Hirst, J., *Carmichael, S.K., *Fisher, R.G.M., *Wegmann, K.W., and Monteleone, B. (2004) Proterozoic metamorphism of the Tobacco Root Mountains, Montana, in Brady, J.B., Burger, H.R., Cheney, J.T., and Harms, T.A., eds, Precambrian Geology of the Tobacco Root Mountains, Montana: Geological Society of America Special Paper 377, 105-129.
- Cramer, M.A., Voarino, B., and Baldwin, J.A. (2013) Metamorphic evolution of Precambrian basement in the southern Ruby Range, SW Montana in Geological Society of America Abstracts with Programs, 45, 601.
- De Capitani C. and Petrakakis K. (2010): The computation of equilibrium assemblage diagrams with Theriak/Domino software. American Mineralogist 95:1006-1016
- Harms, T.A., Brady, J.B., Burger, H.R. and Cheney, J.T. (2004) Advances in the geology of the Tobacco Root Mountains, Montana, and their implications for the history of the northern Wyoming Province, in Brady, J.B., Burger, H.R., Cheney, J.T., and Harms, T.A., eds. Precambrian Geology of the Tobacco Root Mountains, Montana: Geological Society of America Special Paper 377, p. 227-243.
- Powell, R. & Holland, T.J.B. 1988 An internally consistent thermodynamic dataset with uncertainties and correlations: 3: application methods, worked examples and a computer program. Journal of Metamorphic Geology 6, 173-204.
- James, H.L. (1990) Plate 1: Geologic map of the Southwestern Ruby Range, Montana in Precambrian Geology and Bedded Iron Deposits of the Southwestern Ruby Range, Montana: US Geological Survey Professional Paper 1495, 44.
- Spear, Frank A., Kohn, Matthew, J., Cheney, John T. (1999) P-T paths from anatectic pelites. Contributions to Mineralogy and Petrology 134: 17-32